ent and nonadherent populations of cells for synthesis of spectrin and other erythrocyte-specific membrane proteins and for decreases in cell volume and condensation of nuclei to see which is correlated with the loss of fibronectin adhesion. It is possible that the appearance of band III protein is itself responsible for the loss of adhesiveness of the differentiated MEL cells. It will also be important to determine whether this phenomenon involves a decrease in the number of fibronectin binding sites on the surface of the differentiated MEL cells.

The relevance of our findings to erythropoiesis in bone marrow remains to be established. However, we note that fibronectin is found in close association with hematopoietic colonies in explant cultures of developing bone marrow (*15*). Bone marrow is also bathed by plasma, which contains the soluble form of fibronectin. It is known that fibronectin promotes cell attachment only when this glycoprotein is adsorbed as part of the substrate (*16*). The fibronectin matrix in bone marrow may anchor differentiating erythroid cells, preventing their premature release into the circulation. If this is true, loss or modification of fibronectin binding sites on the surface of the end-stage cells could underlie their release into the circulation.

VIKRAM P. PATEL
HARVEY F. LODISH

Department of Biology, Massachusetts Institute of Technology, Cambridge 02139

References and Notes

1. J. B. Geiduschek and S. J. Singer, *Cell* **16**, 149 (1979).
2. T. L. Steck, *J. Cell Biol.* **62**, 1 (1974).
3. H. Chang, P. J. Langer, H. F. Lodish, *Proc. Natl. Acad. Sci. U.S.A.* **73**, 3206 (1976).
4. C. G. Gahmberg, M. Jokinen, L. C. Andersson, *Blood* **52**, 379 (1978).
5. V. T. Marchesi, *J. Membr. Biol.* **51**, 101 (1979); D. Branton, C. M. Cohen, J. Tyler, *Cell* **24**, 24 (1981).
6. H. Eisen, R. Bach, R. Emery, *Proc. Natl. Acad. Sci. U.S.A.* **74**, 3898 (1977).
7. F. M. Van Bockxmeer and E. H. Morgan, *Biochim. Biophys. Acta* **584**, 76 (1979); B. T. Pan, R. Blostein, R. M. Johnstone, *Biochem. J.* **210**, 37 (1983).
8. A. H. Reddi, personal communication.
9. R. O. Hynes and K. M. Yamada, *J. Cell Biol.* **95**, 369 (1982); H. K. Kleinman, R. J. Klebe, G. R. Martin, *ibid.* **88**, 473 (1981).
10. C. Friend, W. Scher, J. G. Holland, T. Sato, *Proc. Natl. Acad. Sci. U.S.A.* **68**, 378 (1971); P. A. Marks and R. A. Rifkind, *Annu. Rev. Biochem.* **47**, 419 (1978).
11. E. L. Sabban, D. D. Sabatini, V. T. Marchesi, M. Adesnik, *J. Cell. Physiol.* **104**, 261 (1980).
12. A. Bendetto, C. Amici, W. Djaczenko, S. Zamiratti, M. G. Santoro, *Exp. Cell Res.* **134**, 219 (1981).
13. H. K. Kleinman, E. B. McGoodwin, S. I. Rennard, G. R. Martin, *Ann. Biochem.* **94**, 308 (1979).
14. V. Volloch and D. Housman, *J. Cell Biol.* **93**, 390 (1982).
15. J. Gusella, R. Geller, B. Clarke, V. Weeks, D. Housman, *Cell* **9**, 221 (1976).
16. R. E. Weiss and A. H. Reddi, *J. Cell Biol.* **88**, 630 (1981).
17. F. Grinnell, *Int. Rev. Cytol.* **53**, 65 (1978).
18. MEL cells were grown in suspension culture in Dulbecco's modified Eagle medium (DMEM) supplemented with 13 percent (by volume) heat-inactivated fetal bovine serum. CHO and HepG2 cells were grown as monolayers in Ham's F-12 medium and DMEM, respectively, both supplemented with serum as above. The cells were detached with 0.2 percent trypsin (Gibco) and washed three times with Hanks buffered salt solution containing soybean trypsin inhibitor (50 μg/ml). All cells were washed once and assayed for attachment in their respective growth medium. Attachment of CHO and HepG2 cells was measured in the presence of soybean trypsin inhibitor (25 μg/ml).
19. Fibronectin was purified from human plasma as described by E. Engvall and E. Ruoslathi [*Int. J. Cancer* **20**, 1 (1977)], except that the gelatin-sepharose column was sequentially washed with 1*M* NaCl and 1*M* urea before fibronectin was eluted with 3*M* urea (J. Gardner, personal communication). The eluted fibronectin was ~ 98 percent pure, as measured by sodium dodecyl sulfate–gel electrophoresis. Fibronectin and laminin were applied to Falcon 1008 plastic petri dishes (diameter, 35 mm) essentially as described by E. Ruoslathi and E. G. Hayman [*FEBS Lett.* **97**, 221 (1979)] and by E. Engvall [*Methods Enzymol.* **70**, 419 (1980)]. Collagen type I (Flow) and collagen type IV fibers were reconstituted from solution onto the dishes by exposure to ammonium hydroxide vapors for a few minutes at 24°C, producing a firm adherent gel [T. Elsdale and J. Bard, *J. Cell Biol.* **54**, 626 (1972)]. Typically, dishes were coated with protein substrates just before the cell attachment assay.
20. J. M. Owen, A. M. Kissonerghis, H. F. Lodish, *J. Biol. Chem.* **255**, 9678 (1980).
21. We thank H. K. Kleinman for the gifts of laminin, collagen type IV, and antisera against these proteins; J. Gardner for the gift of fibronectin used during the initial phase of this study; D. Housman's group for providing a subclone of the MEL cell line and for invaluable advice on culture conditions used for growth and induction of MEL cells; and D. Nathan for advice and encouragement. We also thank M. Boucher for her everlasting patience in preparing the manuscript.

3 January 1984; accepted 23 March 1984

Dynamic Heterogeneity: Rapid Generation of Metastatic Variants in Mouse B16 Melanoma Cells

Abstract. *The ability of clonally derived lines of B16F1 and B16F10 melanoma cells to form experimental metastases in C57BL mice after intravenous injection was examined. Luria-Delbruck fluctuation analysis was applied to the results obtained with parallel subclones grown to small population sizes before testing for metastatic ability. The analysis demonstrated that variant cells capable of forming experimental metastases were generated in B16F1 cell populations at an effective rate of about* 1.3×10^{-5} *per cell per generation while in B16F10 cell populations the effective rate of production was about* 5×10^{-5} *per cell per generation. These results are consistent with a dynamic heterogeneity model of tumor progression. They suggest that the majority of cells in both lines are effectively nonmetastatic and that the higher metastatic ability of the B16F10 population may be due in part to a higher rate of generation of metastatic variants.*

The concept that generation of diversity in a tumor cell population leads to tumor heterogeneity and malignant progression has gained wide acceptance (*1*, *2*). However, the rates at which aspects of this progression occur have been measured in only a few systems (*3*). We recently analyzed clonal isolates of mouse KHT fibrosarcoma cells grown to small, defined population sizes (*4*). Most of the cells were effectively nonmetastatic (as defined by lung tumor formation after intravenous injection of KHT cells), and metastatic variants were generated spontaneously at unexpectedly high rates. Furthermore, such variants apparently were lost at even higher rates when the cells were grown in vitro or in vivo (*5*). These findings indicate that one feature of metastatic disease is a rapid turnover of metastatic variants and that the frequency of such variants in the population is determined by the effective rates of their generation and loss. This concept has been termed the dynamic heterogeneity model of tumor progression (*4*). In this study we examined whether such a model, which had been studied only in KHT fibrosarcoma cells, is also applicable to the widely studied murine B16 melanoma tumor. Specifically, we measured the rates of generation of metastatic variants in the relatively poorly metastatic B16F1 line and the more highly metastatic B16F10 line isolated by Fidler (*6*).

The rate of generation of metastatic variants was measured by growing clonal isolates to defined cell numbers before analysis. When variants are generated stochastically during the growth of a clone, a critical population size needs to be attained before there is a significant probability that variants will occur in that population. The critical population size is related to the rate of variant generation, as illustrated by the analysis of drug-resistant variants by Goldie and Coldman (*7*). For measurement of rapid rates the ability to monitor and grow cells to a predetermined small population size is crucial; thus we used an in situ monitoring procedure to identify clones grown to appropriate sizes for analysis (Fig. 1).

If the generation of metastatic variants

in the B16 melanoma system is similar to that previously determined for KHT cells, then clones grown to approximately 10^5 cells would have just reached the critical size and a significant number of clones would contain no detectable metastatic variants. On the other hand, clones grown for six to seven more generations (to 10^7 cells) would be well past the critical size and all or almost all the clones would contain at least some metastatic variants. The results of an experiment to test this prediction are shown in Fig. 2. When clones derived from B16F1 cells were grown to a population of 5×10^5 cells, five-ninths of them contained no detectable metastatic variants as determined by the experimental metastasis assay, and the clones that did contain metastatic variants produced only a few lung tumors per mouse. When clones were grown to 10^7 cells, all contained metastatic variants. Furthermore, a wide range was observed among the clones, with some producing a median of nearly 100 lung tumors per mouse. These results are consistent with the dynamic heterogeneity model and indicate that most clonable B16F1 cells express a nonmetastatic phenotype and that metastatic variants are generated at a relatively high rate during clonal expansion.

A series of cloning experiments similar to the one described above was performed with B16F1 and B16F10 cells. The generation rates of variant cells capable of forming experimental metastases were calculated by using Luria-Delbruck fluctuation analysis, as described earlier (*4*) for KHT fibrosarcoma cell lines (Table 1). In the B16F1 line the rate at which effective metastatic variant cells were generated was approximately 1×10^{-5} per cell per generation, while in the B16F10 line the rate was about four times higher ($P < 0.01$). To confirm the higher generation rate of metastatic variant cells in line B16F10, we grew clonal isolates of B16F10 cells close to the critical population size predicted by the higher rate to determine whether a significant number of clones without metastatic variant cells would be observed (experiment 11 in Table 1). The clonal isolates were grown to a population size of only 5×10^4 cells, and essentially all the cells from each clone were injected into a single mouse. In this experiment no metastatic variants were observed in more than 20 percent of the clones, yielding an effective rate of variant production of 7.3×10^{-5}. A similar experiment with B16F1 cells (experiment 6 in Table 1) yielded a rate about three times lower, consistent with the other studies. These results support the hypothesis that most of the cells in line B16F10 are effectively nonmetastatic and that the higher metastatic ability of line B16F10 than B16F1 may be due in part to a higher rate of generation of metastatic variant cells.

The high generation rates of metastatic variants measured in this and previous studies (*4, 8*) may cast light on the mechanism responsible for such rapid changes. Their spontaneous nature raises the possibility of a genetic origin. Genetic changes with generation and loss rates as rapid as those described here were recently demonstrated in markers associated with gene amplification (*9*). It may be significant that the

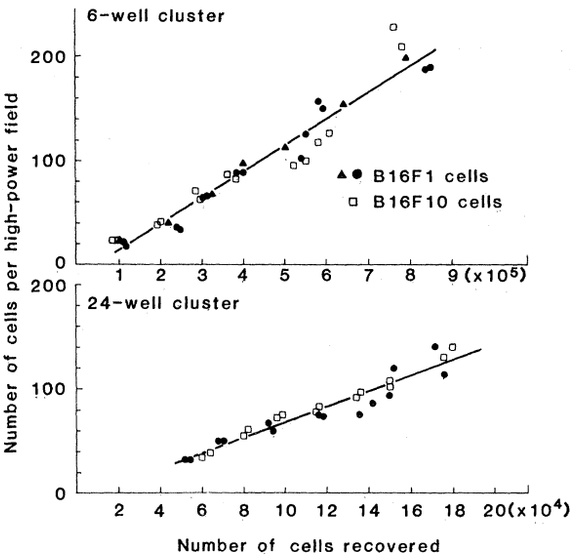

Fig. 1. Relation between the mean number of cells per microscope field and the number of cells recovered by trypsinization for cells growing in Linbro tissue culture clusters. B16F1 or B16F10 cells were seeded at different concentrations in six or 24-well Linbro clusters in α–minimum essential medium (α-MEM) plus 10 percent fetal calf serum (α-MEM-S) and incubated for 3 to 6 hours. When the cells had attached, the number of cells in the monolayers was estimated by counting the cells in three microscope fields (×320) chosen at random. Cells in the individual wells were then trypsinized to prepare a suspension and suspensions from the individual wells were counted with a Coulter counter. The number of cells recovered by trypsinization was not significantly different from the number originally seeded. The means of the individual cell counts in the microscope fields are shown by squares (B16F10) or circles (B16F1). The results of a similar experiment done 3 to 4 months earlier with B16F1 cells are shown by triangles. The individual wells have approximate surface areas of 200 mm^2 (24-well cluster) and 900 mm^2 (six-well cluster). By growing cells in containers with different cell surface areas, it was possible to obtain clonal populations with different cell numbers and yet a relatively constant final cell density, which avoids potential variations that may be dependent on cell density (*17*).

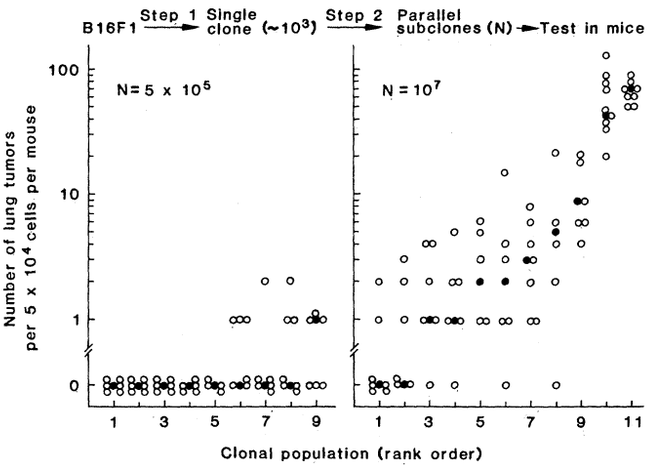

Fig. 2. Number of lung metastases observed in mice injected with different clones of B16F1 cells. Cells were cloned by limiting dilution into 24-well Linbro tissue culture clusters in α-MEM-S. A well containing a single clone was identified, and when the clone reached approximately 10^3 cells it was trypsinized and the process of cloning by limiting dilution was repeated with the suspension obtained. Wells containing individual colonies were again identified, and after a number of days the colonies were trypsinized to allow transfer of the cells to six-well Linbro tissue culture clusters or to a T75 flask. The clones were then allowed to grow until they reached a total population of approximately 5×10^5 cells (Linbro wells) or approximately 10^7 cells (T75 flasks). The cells were then trypsinized, resuspended in α-MEM-S, and injected into groups of C57BL mice (5×10^4 cells per mouse). For clones grown to approximately 5×10^5 cells the cell number was estimated by using the results shown in Fig. 1 so that essentially all the cells could be injected into mice. After 21 days the mice were killed and examined for metastases. Open circles show the number of lung metastases observed in the individual mice injected with cells from the different clones. Closed circles show the median mouse for each clone.

appearance of double-minute chromosomes, a feature associated with unstable gene amplification (*10*), is commonly observed in progressed human tumor cells (*11*). Moreover, the concept that amplification of certain genes or overproduction of certain gene products is closely associated with malignancy has gained wide support (*12*).

Several general models of the metastatic process have been reviewed by Weiss (*13*). They are the random survival model, the (stable) preexisting metastatic phenotype model, the site-induced modulation model, and the transient metastatic compartment model. The results presented here provide data that can be used to test the validity of these and other models. Superficially, our results are most compatible with the predictions of the transient metastatic compartment model. However, this model is general and is not genetic in its original concept. The dynamic heterogeneity model we propose on the basis of our quantitative analyses suggests that a genetic mechanism is involved in the generation of metastatic variants.

Considerable efforts have been made to isolate variant cell lines with increased metastatic ability so that cellular and biochemical changes responsible for the metastatic phenotypes can be more clearly defined (*2, 14*). Such efforts have largely proved disappointing, since in many cases the metastatic lines were unstable, losing their phenotype within a short time (*2*). In other cases a relatively stable population difference in metastatic ability has been observed, as with lines B16F1 and B16F10, but identification of relevant cellular and biochemical differences has remained elusive (*14*). The present findings provide a consistent explanation for these observations by establishing the following points:

1) In lines B16F1 and B16F10 most of the cells are similar, being effectively nonmetastatic.

2) Metastatic variant cells are generated at high rates.

3) The effective frequencies of metastatic variants in many established populations are low, being on the order of 10^{-2} to 10^{-4} (*4, 6, 15*). Because the frequency is dependent on a ratio of the rates of generation and loss, the metastatic variant cells must be lost at rates higher than the generation rates (*5*).

4) The difference in metastatic ability between lines B16F1 and B16F10 may result at least in part from an increased effective rate of generation of metastatic variant cells in line B16F10.

Points 1 and 3 suggest that biochemical and cellular differences associated with metastatic ability have been difficult to detect between lines B16F1 and B16F10 because most of the cells are similar. Points 2 and 3 provide an explanation for the apparent instability of many metastatic lines, since the metastatic ability of such lines may be determined by rapid turnover of a subpopulation of metastatic variant cells. It seems possible that the size of this subpopulation can vary dramatically depending on different factors. In this context, the observation that clonal interactions and cell morphology (*2, 16*) affect the expression of the metastatic phenotype in B16 melanoma cells deserves further investigation. Point 4 explains how certain lines, such as B16F10, maintain increased metastatic ability despite their heterogeneous nature. This phenomenon seems to result from an increased effective rate of generation of metastatic variant cells. Thus, it appears that the dynamic heterogeneity model proposed for KHT fibrosarcoma cells (*4*) applies to the B16 melanoma system and that it may provide a basis for further investigation of the metastatic process.

R. P. HILL
A. F. CHAMBERS*
V. LING
Ontario Cancer Institute and Department of Medical Biophysics, University of Toronto, Toronto, Ontario, Canada M4X 1K9
J. F. HARRIS*
Department of Surgery, Wellesley Hospital, University of Toronto

Table 1. Summary of rate analysis. Clones were obtained by using the procedure outlined in the figure legends. Cell numbers were estimated from microscope counts except in experiments 1, 2, 7, 8, and 12, in which clones were transferred to and grown in T75 flasks and cell concentration was determined with a Coulter counter. The number of parallel clones and the final number of cells are recorded for each experiment. Parallel clones were injected intravenously in seven to eight mice in all experiments except 6 and 11, in which one mouse per clone was assessed. The number of cells injected per mouse was 5×10^4 in experiments 1 to 5 and 8 to 10 and 3×10^4 in experiments 6, 7, 11, and 12. In all experiments except 2 and 5, clones were obtained from mass cultures of B16F1 or B16F10 cells. In experiments 2 and 5, clones were obtained from a subclone of B16F1 that had grown to approximately 10^3 cells.

Experiment	C*	P_0†	N‡ ($\times 10^{-5}$)	M/N§ ($\times 10^4$)	μ‖ ($\times 10^5$)
			Line B16F1		
1	9	0	200	1.5	1.2
2	11	0	100	3	2.2
3	9	0	5	0.4	0.6
4	8	0	5	0.96	1.3
5	9	0.56	5	0.04	0.1 (0.1)
6	51	0.33	0.5	2.2	2.8 (2.2)
7	6	0	200	0.4	0.38
			Line B16F10		
8	9	0	200	7.4	5
9	9	0	5	4.2	4.4
10	7	0	5	2.8	3.2
11	48	0.21	0.5	6.7	7.3 (3.1)
12	6	0	200	8.8	6

*C is the number of parallel clones. †P_0 is the fraction of parallel clones with no observed lung colonies. In experiment 12, 42 of 42 mice had >1 lung tumor. With this result the hypothesis that the P_0 observed in experiment 11 arose by chance was rejected ($P < 0.001$, χ^2 test). ‡N is the number of cells to which each clone was grown. §M/N is the observed mean frequency of lung tumors per cell. ‖The effective rate of formation of lung tumors, μ, was calculated with $\mu \ln(3.46\mu NC) - (M/N) \ln 2 = 0$. In experiments 5, 6, and 11 the Poisson method was also used to calculate μ [$= -(\ln P_0)/N$], as shown in brackets. The effective rates observed for line B16F1 are significantly lower than the effective rates observed for line B16F10 ($P < 0.01$, Mann-Whitney U-test or Student's t-test for the difference between the means). The calculation of effective rate assumes that the metastatic variant cells are 100 percent efficient in forming lung metastases (*4*). It is not possible to measure this efficiency directly, but if it is less than 100 percent then the actual rate of variant production is correspondingly higher.

References and Notes

1. L. Foulds, *Neoplastic Development* (Academic Press, New York, 1969), vol. 1; P. C. Nowell, *Science* **194**, 23 (1976).
2. L. Weiss, *Pathobiol. Annu.* **10**, 51 (1980); I. J. Fidler and I. R. Hart, *Science* **217**, 998 (1982); G. Poste and R. Greig, *Invasion Metas.* **2**, 137 (1982); G. H. Heppner and B. E. Miller, *Cancer Metas. Rev.* **2**, 5 (1983).
3. J. C. Barrett and P. O. P. Ts'o, *Proc. Natl. Acad. Sci. U.S.A.* **75**, 3761 (1978); D. G. Thomassen and R. DeMars, *Cancer Res.* **42**, 4054 (1982); V. Ling, in *Drugs and Hormone Resistance in Neoplasia*, N. Bruchovsky and J. H. Goldie, Eds. (CRC Press, Miami, 1982), pp. 1–19.
4. J. F. Harris, A. F. Chambers, R. P. Hill, V. Ling, *Proc. Natl. Acad. Sci. U.S.A.* **79**, 5547 (1982).
5. A. F. Chambers, J. F. Harris, V. Ling, R. P. Hill, *Invasion Metas.*, in press.
6. I. J. Fidler, *Nature (London) New Biol.* **242**, 148 (1973); *Cancer Res.* **35**, 218 (1975).
7. J. H. Goldie and A. J. Coldman, *Cancer Treat. Rep.* **63**, 1727 (1979).
8. A. E. Lagarde, *Invasion Metas.* **3**, 52 (1983).
9. R. N. Johnston, S. M. Beverley, R. T. Schimke, *Proc. Natl. Acad. Sci. U.S.A.* **80**, 3711 (1983).
10. R. J. Kaufman, P. C. Brown, R. T. Schimke, *ibid.* **76**, 5669 (1979).
11. P. E. Barker and T. C. Hsu, *J. Natl. Cancer Inst.* **62**, 257 (1979).
12. G. Klein, *Nature (London)* **294**, 313 (1981); M. L. Pall, *Proc. Natl. Acad. Sci. U.S.A.* **78**, 2465 (1981); D. L. George and V. E. Powers, *ibid.* **79**, 1597 (1982); R. A. Weinberg, *Adv. Cancer Res.* **36**, 149 (1982); K. Alitalo, M. Schwab, C. C. Lin, H. E. Varmus, J. M. Bishop, *Proc. Natl. Acad. Sci. U.S.A.* **80**, 1707 (1983); J. M. Bishop, *Annu. Rev. Biochem.* **52**, 301 (1983).
13. L. Weiss, in *Brain Metastasis*, L. Weiss, H. A.

Gilbert, J. B. Posner, Eds. (Hall, Boston, 1980), p. 30; *Invasion Metas.* **3**, 193 (1983).
14. G. A. Turner, *Invasion Metas.* **2**, 197 (1982).
15. A. F. Chambers, R. P. Hill, V. Ling, *Cancer Res.* **41**, 1368 (1981); L. Weiss, in *Tumor Invasion and Metastasis*, L. A. Liotta and I. R. Hart, Eds. (Nijhoff, Boston, 1982), p. 81.
16. A. Raz and A. Ben-Ze'ev, *Science* **221**, 1307 (1983).
17. H. B. Bosmann and A. Lione, *Biochem. Biophys. Res. Commun.* **61**, 564 (1974).

18. We thank R. F. Kuba and M. Naik for technical assistance. B16F1 and B16F10 cells were the kind gift of I. J. Fidler. Supported by the National Cancer Institute of Canada, the Medical Research Council of Canada, and the Ontario Cancer Treatment and Research Foundation.
* Present address: Ontario Cancer Foundation, London Clinic, London, Ontario, Canada N6A 4G5.

5 December 1983; accepted 29 February 1984

The Respiratory Sinus Arrhythmia: A Measure of Cardiac Age

Abstract. *A method developed for quantifying respiratory sinus arrhythmia (RSA) during voluntary cardiorespiratory synchronization relies on computer-assisted rhythmometric cosinor analysis of instantaneous heart rate data. The RSA was present in all subjects tested, even those at advanced ages. The amplitude of the RSA falls approximately 10 percent per decade. An individual with a transplanted heart and one with severe diabetic neuropathy each had resting RSA values that were normal for their ages. The shape and amplitude of the RSA during voluntary cardiorespiratory synchronization may reflect the suppleness of the heart and its response to rhythmically changing intrathoracic pressure and the subsequent ebb-and-flow of venous return. Our technology allows objective quantitative assessment of the biologic age of the heart and also the effect of any drug, disease, or behavior that affects the RSA.*

In 1733, Hales observed that changes in blood pressure and pulse were related in a regular manner to the respiratory pattern in the horse (*1*). In 1846, Ludwig's invention of the kymograph allowed his observation of the regular quickening of pulse with inspiration and slowing with expiration in the dog (*2*). Medical students have been taught for more than a century that this regular irregularity of heart beat disappears with advancing age (*3*). Since few biologic phenomena disappear abruptly, it seemed to us that the inexactitude of clinical methods for detecting the respiratory sinus arrhythmia (RSA) might be responsible for its apparent disappearance. Furthermore, any cardiovascular physiologic end point that changes predictably with advancing age is of potential major interest.

Quantitative statistical analysis of this phenomenon has been made possible by two discoveries. In 1963, a voluntary coupling system that allows the subject to couple breathing pattern to heart rate (*4–6*) was developed. The coordination of pulse and breathing allows straightforward analysis of resultant instantaneous heart rate data. Since prior statistical evaluations of the RSA have relied upon the assessment of heart rate variance in the unsynchronized state, only very gross, usually pharmacologically induced, differences have been perceptible (*7, 8*). In 1972, development of the single cosinor method of analysis made accurate quantification and statistical analysis of rhythmic biological functions practical (*9*). Spectral analysis of heart rate periodicity and the variance of periods within a window encompassing the respiratory frequency has been the most widely used alternative methodology (*10, 11*).

Modern microcomputer technology has allowed us to investigate the reproducibility of this physiologic parameter and to quantify the effect of advancing age. We studied a group of 25 healthy subjects, ranging in age from 20 to 82, who visited the cancer detection clinic for routine screening examination. We also investigated RSA mechanisms in patients selected because of their unique cardiovascular anatomy or disease state.

The principal features of this system include a pulse sensor; a current discriminator and clock to count and time successive electrical impulses generated by the pulse transducer that correspond to sensed heartbeats and determine an instantaneous heart rate; and driver circuits to relay the desired ratio pattern of visual and auditory signals displayed through a cathode ray tube that advise the subject to inhale and exhale for each of the preselected number of heartbeats. This system is closed when the subject voluntarily breathes according to the transmitted instructions. The subject's ability to follow visual signals is quantitatively verified by a mouthpiece-mounted thermistor which detects breathing (Fig. 1).

All data in this report were obtained using the ratio of two beats for inspiration followed by three beats for expiration, but any desired ratio may be studied in this way. The beat-to-beat interval

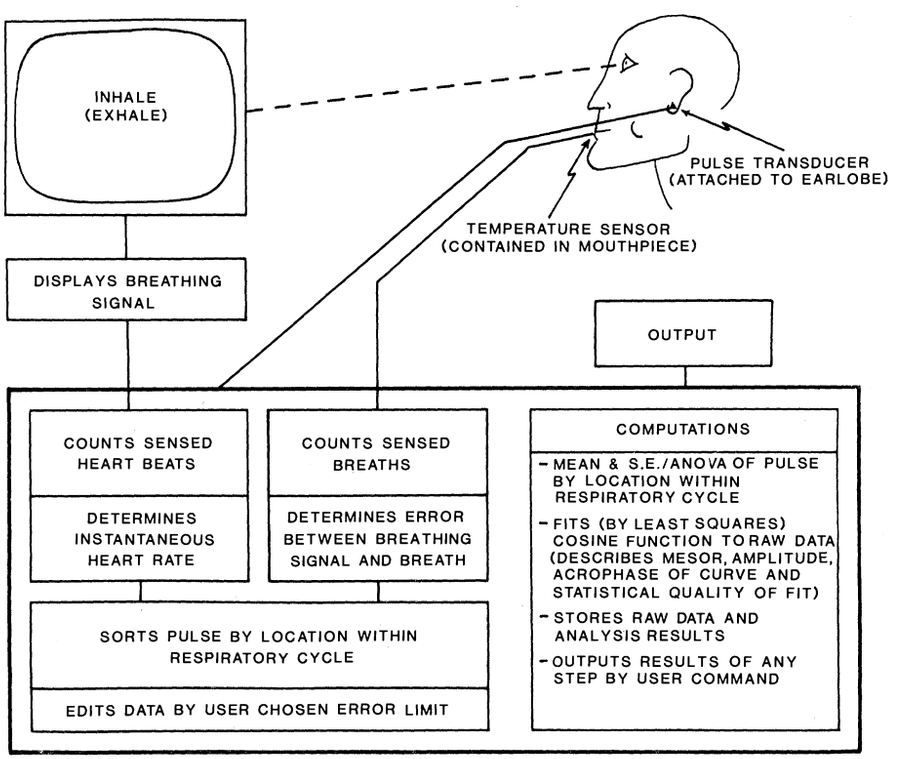

Fig. 1. The necessary components and basic function of the Sine-o-graph pulse monitor, including a pulse sensor to count beats and determine instantaneous heart rate, a respiration sensor for discrimination of inhalation and exhalation and sorting with pulse, interactive software and display of inhale and exhale signals, a statistical package, and a unit for hard copy output.